Bifurcation bridges between external-cavity modes lead to polarization self-modulation in vertical-cavity surface-emitting lasers

M. Sciamanna,[1] T. Erneux,[2] F. Rogister,[1] O. Deparis,[1] P. Mégret,[1] and M. Blondel[1]

[1]*Service d'Electromagnétisme et de Télécommunications, Faculté Polytechnique de Mons, Boulevard Dolez 31, B-7000 Mons, Belgium*
[2]*Optique Nonlinéaire Théorique, Université Libre de Bruxelles, Campus Plaine, Code Postal 231, B-1050 Bruxelles, Belgium*

We analyze the bifurcation mechanism responsible for the experimentally observed polarization self-modulation (PSM) in a vertical-cavity surface-emitting laser subject to optical feedback. We show that closed branches of time-periodic intensity solutions connecting distinct external-cavity modes (ECMs) exhibit PSM. Along these bridges, the linearly polarized components of the optical field oscillate in antiphase and with a frequency close to the difference between two ECM frequencies. A beating mechanism between stable ECMs then explains the PSM phenomenon. Our results also substantiate recent theoretical studies of edge-emitting lasers subject to optical feedback.

Vertical-cavity surface-emitting lasers (VCSELs) generally emit a linearly polarized light along one of two orthogonal directions (called x and y) [1]. High-speed switching between these two polarizations has been experimentally demonstrated when submitting the VCSEL to an optical feedback through a quarter-wave plate whose optical axis is oriented at 45° according to the VCSEL eigenaxes [2–6]. After each round trip in the external cavity the light reentering the laser cavity is rotated by 90°. The light is then observed to switch periodically in antiphase between x- and y-linearly-polarized components, at a period close to but slightly larger than twice the external cavity round-trip time. This so-called *polarization self-modulation* (PSM) may lead to an all optical source of high-frequency signals [7].

Experimental studies [4–6] suggest that PSM is related to a beating between two external cavity modes (ECMs) that are linearly polarized along the eigenaxes of the compound cavity. However, none of the previous reports have identified the dynamical instability leading to PSM and the beating mechanism is still unknown.

In previous work [8], we have determined bifurcation diagrams from direct integration of rate equations. Branches of stable PSM solutions were followed as we increase the feedback rate and we have shown that other solutions than PSM were possible depending on the external cavity length. But our numerical study allowed us to compute only stable solutions. Recent studies of simpler delayed semiconductor laser systems [9,10] have shown, however, that unstable solutions might play a key role in the dynamics. For this purpose, they have used a continuation package for delay differential equations [11] that follows both stable and unstable steady and time-periodic solutions. We have adapted this method to our VCSEL problem in order to have a better understanding of the bifurcation mechanisms leading to PSM. Our numerical study complements a linear stability analysis of the ECM solutions revealing their Hopf bifurcation points. As the feedback rate is progressively increased from zero, we find closed branches of stable and unstable pulsating intensity solutions (bridges) which connect these Hopf bifurcation points. They represent smooth transitions between ECMs that are linearly polarized along the two eigenaxes of the

compound cavity. A beating mechanism between the two interacting ECMs then explains the PSM phenomenon. In previous work, only partially stable bridges were reported between a mode (stable ECM) and an antimode (unstable ECM) [10] but our results show that largely stable bifurcation bridges between modes are possible in a delayed semiconductor laser system. They revive the interest in finding fully stable bridges in edge-emitting lasers and they substantiate the idea that a bifurcation bridge is a generic phenomenon for high-frequency pulsating intensities in semiconductor lasers subject to optical feedback.

Our numerical simulations use the following rate equations [5,8]:

$$\frac{dE_{x,y}}{ds} = \frac{1}{2}(1+i\alpha)[(1+2Z)F_{x,y}-1]E_{x,y}$$
$$+ \eta E_{y,x}(s-\theta)\exp(-i\phi_f), \quad (1)$$

$$T\frac{dZ}{ds} = P - Z - (1+2Z)(F_x|E_x|^2 + F_y|E_y|^2), \quad (2)$$

where

$$F_{x,y} = 1 - \varepsilon_{s,c}\left(|E_x|^2 - \frac{P}{2}\right) - \varepsilon_{c,s}\left(|E_y|^2 - \frac{P}{2}\right). \quad (3)$$

E_x and E_y are the slowly varying linearly polarized components of the optical field. Z is the carrier density. s is the time t divided by the photon lifetime τ_p, α is the phase-amplitude coupling coefficient, and T is the ratio of the carrier lifetime τ_s to τ_p. η is the feedback rate normalized by τ_p^{-1} and θ is the round-trip time in the external cavity, $\tau \equiv 2L/c$, divided by τ_p (L is the external cavity length and c is the speed of light). ϕ_f is the feedback phase. P is the injection current above threshold. Finally, F_x and F_y are two gain compression functions, with ε_s (ε_c) the self- (cross-)compression coefficient. Equations (1)–(3) have been simulated numerically using $T=1000$, $\alpha=3$, $\varepsilon_s=0.02$, and $\varepsilon_c=0.04$. Typical values for ε_s range between 0.01 and 0.1 [12,13] and ε_c is typically a factor of 2 larger than ε_s [12]. We consider

$P = 0.4$ and $\theta = 100$. If $\tau_p = 1$ ps, this means that $\tau = 100$ ps or $L = 1.5$ cm. For simplicity, we assume $\phi_f = 0$. η is our bifurcation parameter.

The steady state intensity solutions of Eqs. (1)–(3) are of the form

$$E_x = X \exp[i(\omega s + \phi_x)],$$

$$E_y = Y \exp[i(\omega s + \phi_y)], \tag{4}$$

where the amplitudes X and Y and the phases ϕ_x and ϕ_y are constant. Introducing Eq. (4) into Eqs. (1)–(3) leads to five equations for X, Y, Z, ω, and $\Delta \equiv \phi_x - \phi_y$ which can be solved analytically.

Steady state solutions exhibiting $X \equiv Y$ correspond to single ECMs similar to those of the Lang-Kobayashi (LK) equations for edge-emitting lasers [14]. The symmetry of the laser equations allows two types of ECM, namely, the *LK ECMs* ($\Delta = 0$) and the *anti-LK ECMs* ($\Delta = \pi$). The ECM frequencies satisfy the transcendental equation

$$\omega = -\eta[\alpha \cos(\phi_f + \omega\theta + \Delta) + \sin(\phi_f + \omega\theta + \Delta)], \tag{5}$$

while $X = Y$ is obtained by solving the following quadratic equation for X^2:

$$0 = -4(\varepsilon_s + \varepsilon_c)[-1 + 2\eta\cos(\phi_f + \omega\theta + \Delta)]X^4 + \Big\{ -(\varepsilon_s + \varepsilon_c)(1 + 2P) + 4[-1 + 2\eta\cos(\phi_f + \omega\theta + \Delta)]$$

$$\times \Big[1 + (\varepsilon_s + \varepsilon_c)\frac{P}{2}\Big]\Big\}X^2 + (1 + 2P)\Big[1 + (\varepsilon_s + \varepsilon_c)\frac{P}{2}\Big] - 1 + 2\eta\cos(\phi_f + \omega\theta + \Delta). \tag{6}$$

Finally, Z is related to X by

$$Z = \frac{P - 2F_x X^2}{1 + 4F_x X^2}. \tag{7}$$

Because of the value of Δ, the ECMs correspond to a linearly polarized light aligned with one of the two eigenaxes of the compound cavity. These eigenaxes are aligned with the optical axes of the quarter-wave plate, which are at $\pm 45°$ according to the VCSEL eigenaxes (x and y) [4,6].

Steady states with $X \neq Y$ are also possible but only under the condition $\epsilon_c > \epsilon_s$. This condition is also found relevant for the time-periodic solutions that we describe below. Unlike the ECMs, the phase difference Δ depends on η and is in general different from π. These solutions are elliptically polarized steady states (EPSSs).

Figure 1(a) shows $I_x \equiv X^2$ for the ECMs as a function of η. The LK and anti-LK ECMs are shown in black and gray, respectively. Except for the first ECM which emerges at $\eta = 0$, all the ECMs appear in pairs through saddle-node bifurcations. One of the ECMs appearing from this bifurcation can be stable and is called the "mode" while the other one is always unstable and is called the "antimode" [15]. The antimodes correspond to the low intensity part of each branch of steady states. Two branches of EPSSs are also shown in Fig. 1(b). They appear at zero feedback rate and disappear through a pitchfork bifurcation at $\eta \sim 0.006$. It can be shown analytically that the EPSSs exist only for low values of η.

We next determine the possible Hopf bifurcation points. To this end, we use the continuation package of Ref. [11]. Hopf bifurcation points can be classified into either stable or unstable points. Stable Hopf bifurcation points mark the change of stability of a steady state and lead to either a

subcritical (unstable) or a supercritical (stable) time-periodic intensity solution. By contrast, unstable Hopf bifurcation points do not modify the steady state stability. Figure 1(a) indicates that the laser admits stable high-intensity steady state branches which are sequentially LK and anti-LK modes. The arrows in Fig. 1(a) identify stable Hopf bifurcation points from which emerge supercritical periodic branches. Subcritical branches from stable Hopf bifurcation points and branches emerging from unstable Hopf bifurcation points are determined by our numerical continuation method. These unstable branches play an important role in the bifurcation diagram. They connect supercritical periodic branches, meaning a change of stability through a secondary bifurcation. These closed branches connecting Hopf bifurcation points located on nearby but distinct ECMs are called bridges [10]. Physically, these bridges can be considered as mixed ECM solutions [10,16] of the form

$$E_x \simeq X_1 \exp[i(\omega_1 s + \phi_{x1})] + X_2 \exp[i(\omega_2 s + \phi_{x2})],$$

$$E_y \simeq X_1 \exp[i(\omega_1 s + \phi_{y1})] + X_2 \exp[i(\omega_2 s + \phi_{y2})]. \tag{8}$$

The two amplitudes X_1 and X_2 are functions of η. $X_1 = 0$ ($X_2 = 0$) at the Hopf bifurcation point of mode 2 (mode 1). By contrast with the single ECM solutions (4), the intensities $|E_x|^2$ and $|E_y|^2$ are now pulsating in time with a frequency given by $|\omega_1 - \omega_2|$, meaning a beating between ECMs.

Typical bridges are shown in Fig. 2 and illustrate different types of connections. In the first case [Fig. 2(a)], a periodic branch emerges from a stable Hopf bifurcation point located on an anti-LK mode. As the feedback rate is progressively increased, the amplitude of the oscillations increases until a limit point is reached. The bridge then terminates at a stable
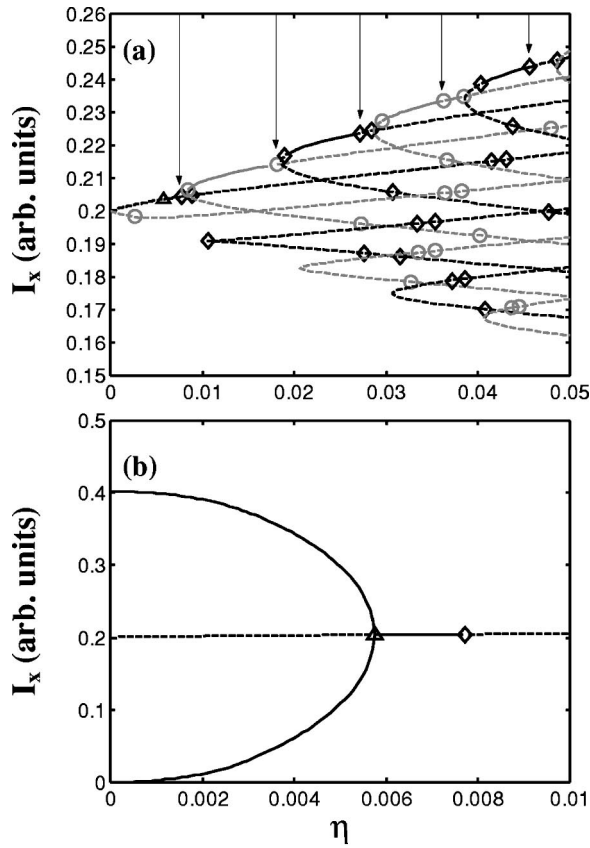
FIG. 1. Steady states of I_x as a function of η, for the parameters specified in the text. (a) represents the LK ECMs and anti-LK ECMs in black and gray, respectively. The $\triangle$ denotes a pitchfork bifurcation point to EPSS solutions shown in (b), for clarity. $\diamond$ and $\bigcirc$ correspond to LK and anti-LK Hopf bifurcation points. Stable and unstable branches are shown by solid and dashed lines, respectively. The arrows indicate supercritical Hopf points.

FIG. 2. Enlargements of parts of Fig. 1(a), showing bifurcation bridges between ECMs. The maximum of I_x is plotted as a function of η. The same symbols as in Fig. 1 mark the Hopf bifurcation points. $\square$ and $\times$ denote limit points of periodic solutions and torus bifurcation points, respectively.

but subcritical Hopf bifurcation point located on a LK mode. This implies a small domain of bistability between this LK mode and the stable branch of periodic solutions. Along the branch of periodic states, the intensities I_x and I_y of the two linearly polarized modes of the VCSEL oscillate in antiphase, as shown in Fig. 3(a). They represent a typical PSM regime. The period of the PSM is larger than but close to twice the external cavity round-trip time. These branches of PSM from moderate to high feedback rates correspond to the experimentally reported PSM [2–6,17]. They exhibit a frequency that results from a beating between two modes, as argued from experimental results [4–6]. Since the ECM frequency depends on the feedback rate, the frequency f_{PSM} of PSM depends on the feedback rate as well. We have indeed observed numerically that f_{PSM} becomes closer to $1/(2\theta)$ as we consider bridges at higher feedback rates. This last point is also in good agreement with experimental findings [17].

In the second case [Fig. 2(b)], a branch of periodic solutions connects a stable Hopf bifurcation point located on a LK mode to an unstable Hopf bifurcation point located on a LK antimode. The periodic solution changes stability thro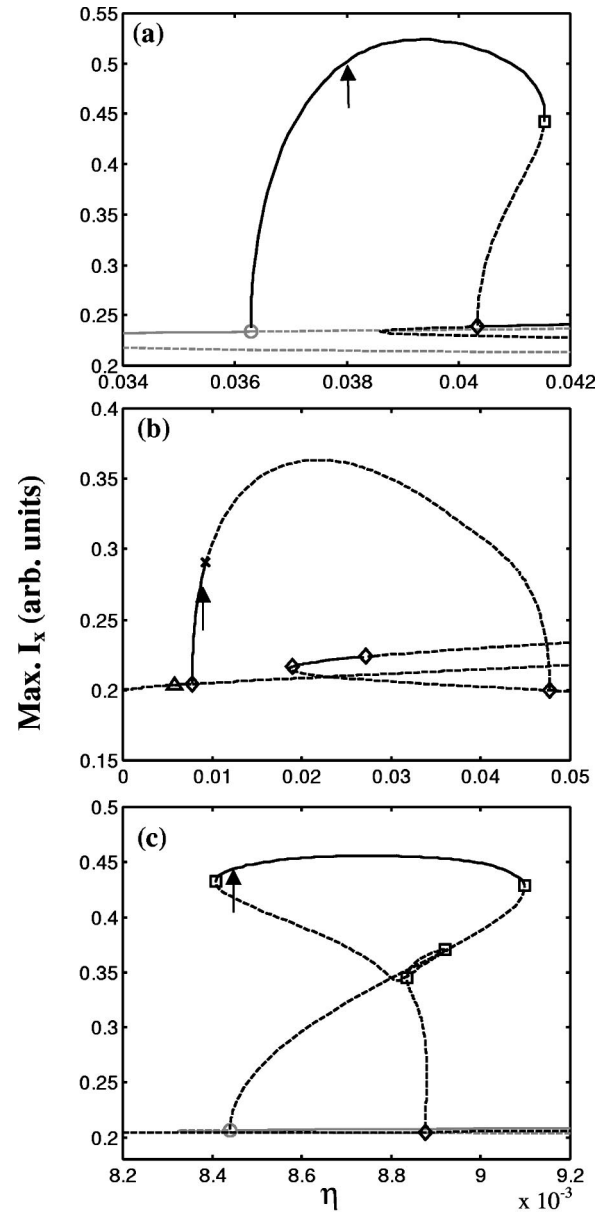ugh a torus bifurcation point. This periodic branch is different from the previous one because $I_x(s) \equiv I_y(s)$ [see Fig. 3(b)].

In the third case [Fig. 2(c)], an isolated branch of periodic solutions is shown to connect a stable (subcritical) Hopf bifurcation point located on an anti-LK mode to an unstable Hopf bifurcation point located on a LK ECM. The stability of the high-intensity part of the twisted branch is determined by two limit points. Along this branch, the two intensities I_x and I_y evolve in antiphase [see Fig. 3(c)], but the period is longer than in Fig. 3(a).

The PSM phenomenon interpreted as a beating between modes persists as we modify the values of the parameters in Eqs. (1)–(3). The bifurcation transition to PSM is also ob-
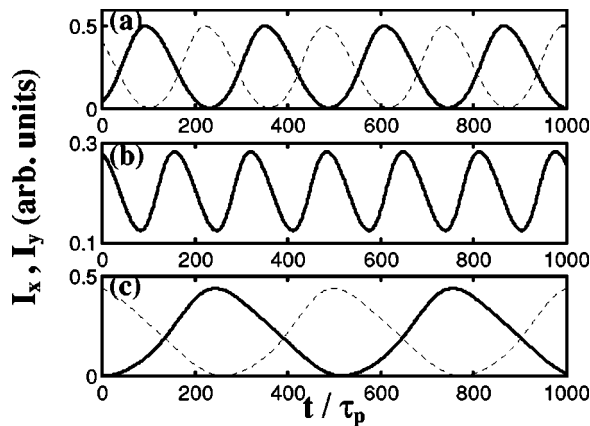
FIG. 3. Time traces of I_x (solid line) and I_y (dashed line) for (a) $\eta = 0.038$, (b) $\eta = 0.009$, (c) $\eta = 0.00842$. They correspond to typical dynamical regimes that are observed along the branches of time-periodic solutions shown in Figs. 2(a)–2(c), respectively (see the arrows in Fig. 2).

served if we consider spin relaxation mechanisms in the VCSEL model [4,18]. Moreover, both complex [4,18] and simplified [5,8] models reproduce qualitatively well the typically reported PSM time traces [2].

Bridges of periodic solutions connecting modes and antimodes have recently been found for edge-emitting lasers subject to optical feedback [10]. For our VCSEL problem, a mode-antimode connection is also possible [Fig. 2(b)]. However, our laser system admits other types of bridge. Of particular interest is the connection between two modes as illustrated in Fig. 2(a). Indeed, by contrast with mode-antimode bridges, a large part of the bridge is now stable and is therefore available experimentally. Furthermore, the two beating ECMs that create PSM are stable and may be identified by recording optical spectra. Mode-mode bridges have not been documented for edge-emitting lasers. This is because the number of ECMs is larger for our laser system compared to the single-polarization Lang-Kobayashi problem. Consequently, more bridges between ECMs may be expected. Bridges between ECMs are also suspected to exist in a double-feedback laser system [19].

In summary, the experimentally observed PSM in an external cavity VCSEL is the result of a beating phenomenon between two distinct but close ECMs. PSM is observed along branches connecting two single ECM Hopf bifurcation points or bridges. These bridges sequentially appear as we increase the feedback rate, suggesting that it is a bifurcation mechanism which may be observed in other delayed laser systems. They motivate further experimental studies of the bifurcation diagram of the PSM regimes as well as theoretical studies in order to determine the conditions for either mode-mode or mode-antimode bridges.

[1] K.D. Choquette, D.A. Richie, and R.E. Leibenguth, Appl. Phys. Lett. **64**, 2062 (1994).

[2] S. Jiang, Z. Pan, M. Dagenais, R.A. Morgan, and K. Kojima, Appl. Phys. Lett. **63**, 3545 (1993).

[3] N. Badr, I.H. White, M.R.T. Tan, Y.M. Young, and S.Y. Wang, Electron. Lett. **30**, 1227 (1994).

[4] F. Robert, P. Besnard, M.L. Chares, and G.M. Stephan, IEEE J. Quantum Electron. **QE-33**, 2231 (1997).

[5] H. Li, A. Hohl, A. Gavrielides, H. Hou, and K.D. Choquette, Appl. Phys. Lett. **72**, 2355 (1998).

[6] G. Ropars, P. Langot, M. Brunel, M. Vallet, F. Bretenaker, A. Le Floch, and K.D. Choquette, Appl. Phys. Lett. **70**, 2661 (1997).

[7] W.H. Loh and C.L. Tang, IEEE J. Quantum Electron. **QE-27**, 389 (1991).

[8] M. Sciamanna, F. Rogister, O. Deparis, P. Mégret, M. Blondel, and T. Erneux, Opt. Lett. **27**, 261 (2002).

[9] D. Pieroux, T. Erneux, T. Luzyanina, and K. Engelborghs, Phys. Rev. E **63**, 036211 (2001).

[10] D. Pieroux, T. Erneux, B. Haegeman, K. Engelborghs, and D. Roose, Phys. Rev. Lett. **87**, 193901 (2001).

[11] K. Engelborghs, DDE-BIFTOOL: a MATLAB package for bifurcation analysis of delay differential equations; http://www.cs.kuleuven.ac.be/˜koen/delay/ddebiftool.shtml.

[12] Y. Takahashi and H. Kawaguchi, IEEE J. Quantum Electron. **QE-36**, 864 (2000).

[13] H. Li, IEEE Photonics Technol. Lett. **8**, 1596 (1996).

[14] R. Lang and K. Kobayashi, IEEE J. Quantum Electron. **QE-16**, 347 (1980).

[15] J. Mork, B. Tromborg, and J. Mark, IEEE J. Quantum Electron. **QE-28**, 93 (1992).

[16] T. Erneux, F. Rogister, A. Gavrielides, and V. Kovanis, Opt. Commun. **183**, 467 (2000).

[17] F. Robert, Ph.D. thesis, Ecole National des Sciences Appliquées et de Technologies, Lannion, France (1997).

[18] C. Masoller and N.B. Abraham, Appl. Phys. Lett. **74**, 1078 (1999).

[19] F. Rogister, D.W. Sukow, A. Gavrielides, P. Mégret, O. Deparis, and M. Blondel, Opt. Lett. **25**, 808 (2000).